

## Endogenous ZAP affects Zika virus RNA interactome

Ahmad Jawad Sabir<sup>a\*</sup>, Nguyen Phuong Khanh Le<sup>b\*</sup>, Prince Pal Singh<sup>b,c\*</sup>, and Uladzimir Karniychuk<sup>b</sup>

<sup>a</sup>Department of Microbiology and Immunology, College of Medicine, University of Illinois, Chicago, IL, USA; <sup>b</sup>Department of Veterinary Biosciences, College of Veterinary Medicine, The Ohio State University, Columbus, OH, USA; <sup>c</sup>School of Public Health, University of Saskatchewan, Saskatoon, Canada

### ABSTRACT

One of the most recent advances in the analysis of viral RNA-cellular protein interactions is the Comprehensive Identification of RNA-binding Proteins by Mass Spectrometry (ChIRP-MS). Here, we used ChIRP-MS in mock-infected and Zika-infected wild-type cells and cells knockout for the zinc finger CCCH-type antiviral protein 1 (ZAP). We characterized 'ZAP-independent' and 'ZAP-dependent' cellular protein interactomes associated with flavivirus RNA and found that ZAP affects cellular proteins associated with Zika virus RNA. The ZAP-dependent interactome identified with ChIRP-MS provides potential ZAP co-factors for antiviral activity against Zika virus and possibly other viruses. Identifying the full spectrum of ZAP co-factors and mechanisms of how they act will be critical to understanding the ZAP antiviral system and may contribute to the development of antivirals.

### ARTICLE HISTORY

Revised 15 July 2024  
Accepted 30 July 2024

### KEYWORDS



Flavivirus; Zika virus; Japanese encephalitis virus; West Nile virus; zinc finger antiviral protein; ZAP; RNA; RNA helicase; interactome

### Introduction


Emerging flaviviruses constantly threaten public health. The National Institute of Allergy and Infectious Diseases classifies flaviviruses – Zika virus, Japanese encephalitis virus (JEV), yellow fever virus (YFV), and West Nile virus (WNV) as a 'Category B Priority', the 2<sup>nd</sup> highest priority of emerging pathogens and biodefense threats. Zika virus caused the human epidemic in 2015 and persists in at least 89 countries. Japanese encephalitis virus causes encephalitis in humans in the Asia-Pacific region [1], with 68,000 annual cases and 15,000 deaths [2]. There is a concern that JEV can be introduced into North America given the large population of amplifying hosts – pigs and wild boars, and susceptible *Culex* mosquitoes [3–5]. Japanese encephalitis virus keeps expanding – the 2022 JEV outbreak in Australia with infections in swine herds, zoonotic transmission, and human deaths was caused by genotype IV which was not associated with outbreaks before [6]. West Nile virus is the most common arthropod-borne virus in the US. In 2022, the US Centers for Disease Control and Prevention reported 1,126 cases and 93 deaths. In 2023, there were 2,406 human cases in the US, including 1,599 neuroinvasive diseases. The rising number of human cases caused by mosquito-borne flaviviruses shows the lack or inefficiency of environmental controls. There are no approved human vaccines for some flaviviruses (i.e. Zika, WNV). Also, there are no licenced antivirals against flaviviruses because of a knowledge gap in cellular pathways controlling infections, including the knowledge gap in interactions of viral RNA with cellular proteins.

High-throughput methods enable global analysis of viral RNA-cellular protein interactions. One of the most recent advances in analysis of viral RNA-cellular protein interactions are the Comprehensive Identification of RNA-binding Proteins by Mass Spectrometry (ChIRP-MS) [7], where interactions between cellular proteins and genomic RNA of several viruses were profiled that advanced the fundamental knowledge of RNA viruses and informed novel antivirals [8–11]. To our knowledge, all these ChIRP-MS studies were done in wild-type cell lines. And comparative ChIRP-MS studies on viral RNA-cellular protein interactions in wild-type and knockout (KO) cell lines are not reported.

The zinc finger CCCH-type antiviral protein 1, also known as ZAP, ZC3HAV1, or PARP13, is a cellular protein with broad antiviral activity. The protein was first characterized to inhibit murine leukaemia virus [12] and later alphaviruses, filoviruses, influenza virus, porcine reproductive and respiratory syndrome virus, hepatitis B virus, human cytomegalovirus, human T cell leukaemia virus type 1, and human immunodeficiency virus-1 [13–23]. The previous study in A549 cells showed JEV sensitivity to ectopic and endogenous ZAP [24]. In the same study, Zika virus was not sensitive to ectopic ZAP; the sensitivity of Zika virus to endogenous ZAP was not tested [24]. Another study using ZAP wild-type and ZAP knockout A549 cells showed that wild-type Zika virus was also not sensitive to antiviral ZAP effects [25]. However, our recent study revealed that Zika virus was sensitive to endogenous ZAP in VERO cells. Specifically, we observed reduced viral RNA, infectious titres, and Zika virus

**CONTACT** Uladzimir Karniychuk  [karniychuk.1@osu.edu](mailto:karniychuk.1@osu.edu)  Department of Veterinary Biosciences, College of Veterinary Medicine, The Ohio State University, 301 Goss Lab, 1925 Coffey Road, Columbus, OH 43210-1093, USA

\*These authors contributed equally.

 Supplemental data for this article can be accessed online at <https://doi.org/10.1080/15476286.2024.2388911>

© 2024 The Author(s). Published by Informa UK Limited, trading as Taylor & Francis Group.

This is an Open Access article distributed under the terms of the Creative Commons Attribution-NonCommercial License (<http://creativecommons.org/licenses/by-nc/4.0/>), which permits unrestricted non-commercial use, distribution, and reproduction in any medium, provided the original work is properly cited. The terms on which this article has been published allow the posting of the Accepted Manuscript in a repository by the author(s) or with their consent.

NS5 protein expression in wild-type cells compared to ZAP knockout cells [26]. This discrepancy may be due to the different cell lines used: previous studies utilized A549 cells derived from human lung cancer tissue [24], while we used VERO cells from a healthy monkey. Antiviral signalling for many cellular proteins can be highly cell-specific [27]. Another factor is the species difference: the previous study used a human cell line, and we used an African green monkey cell line, a possible natural reservoir host of Zika virus [28]. Species-specific ZAP effects are documented [29,30], but comparative studies on ZAP antiviral activity between primates are lacking.

ZAP binds viral RNA and evokes antiviral activity by mediating viral RNA degradation and translational inhibition [31]. It also interacts with various cellular proteins that may act as co-factors, enhancing its antiviral effects [32]. Furthermore, ZAP can augment other antiviral systems [14,26]. To better understand ZAP-viral RNA-cellular protein interactions, here we used Zika virus infection in wild-type and ZAP knockout VERO cells as a model. Specifically, we used ChIRP-MS in mock-infected and Zika-infected wild-type and ZAP knockout cells to characterize ‘ZAP-independent’ and ‘ZAP-dependent’ cellular protein interactomes associated with flavivirus RNA. Our findings suggest that ZAP influences cellular proteins associated with Zika virus RNA.

## Results

### **Endogenous ZAP affects flavivirus infection phenotypes in VERO cells**

While Zika virus was designated as ZAP-resistant in A549 cells [24,25], in our recent study, we showed that Zika virus is sensitive to endogenous ZAP in VERO cells with reduced levels of viral RNA, infectious titres, and NS5 protein expression [26]. Previously, we used the multiplicity of infection (MOI) of 1 for comparative studies in VERO wild-type (VERO-ZAP-WT) and knock-out (VERO-ZAP-KO) cell lines [26]. Here to further confirm antiviral ZAP effects against Zika virus, we conducted comparative studies in the same cells with low MOI 0.01. We also included into the comparative study JEV previously shown to be sensitive to endogenous and ectopically overexpressed ZAP, and WNV with unknown sensitivity to ZAP in VERO cells.

For all flaviviruses, we observed a significant ( $p < 0.0001$ ) reduction in E protein expression in VERO-ZAP-WT compared to VERO-ZAP-KO cells (Figures 1(A,B,E,F,I,J) and Figure S1, S2, S3). All three flaviviruses also showed a considerable reduction of NS5 protein expression in VERO-ZAP-WT compared to VERO-ZAP-KO cells (Figures 1(D,H,L)). The West Nile virus showed comparable intracellular viral RNA loads ( $p = 0.1875$ ) in both VERO-ZAP-WT and VERO-ZAP-KO cells (Figure 1(K)). Consistent with the reduction of E and NS5 protein expression, Zika virus and JEV had significantly higher intracellular RNA loads in VERO-ZAP-KO cells than in VERO-ZAP-WT cells ( $p = 0.0012$  and  $0.0007$ ; Figures 1(C,G)).

Altogether, we confirmed ZAP antiviral effects against JEV and Zika virus, and demonstrated, for the first time to our knowledge, the sensitivity of WNV to ZAP in VERO cells.

Different infection phenotypes in VERO-ZAP-KO than in VERO-ZAP-WT cells suggested ZAP effects mediated via viral RNA binding activity which may involve interactions with other cellular proteins. This motivated us to conduct a ChIRP-MS study to characterize ‘ZAP-independent’ and ‘ZAP-dependent’ cellular protein interactomes associated with Zika virus RNA.

### **ChIRP-MS uncovers ZAP-dependent Zika virus RNA interactome**

To define the ZAP-dependent host protein interactome associated with Zika genomic RNA, we used the RNA-directed proteomic discovery method ChIRP-MS [7–11] in VERO-ZAP-WT and VERO-ZAP-KO cell lines. We crosslinked mock-infected and virus-infected cell lines with formaldehyde to preserve viral RNA–protein complexes and applied biotinylated oligonucleotides (Table S1A) tiling the entire Zika virus RNA to enrich viral RNA–host protein complexes (Figure 2(A)).

For the Zika virus comparative study in VERO-ZAP-WT and VERO-ZAP-KO cells, we used equal MOIs for inoculation to identify ZAP effects on infection phenotypes (Figure 1). However, the different infection phenotypes in VERO-ZAP-WT and VERO-ZAP-KO cells (Figure 1) pose a challenge for ChIRP-MS study where it is essential to induce equal Zika virus RNA loads in both cell lines for an accurate comparison of ZAP-dependent and ZAP-independent interactomes. Thus, before comparing viral RNA–host protein interactions, we tested different Zika MOIs for inoculation of ZAP-WT and ZAP-KO cells to ensure similar viral RNA loads at the time of formaldehyde fixation and accurate comparative ChIRP-MS. For this, we incrementally increased the MOI for VERO-ZAP-WT cells, as Zika virus caused a more aggressive infection in VERO-ZAP-KO cells (Figure 1). The multiplicity of infection 10 for VERO-ZAP-WT cells and MOI 2 for VERO-ZAP-KO cells evoked similar Zika virus loads. To exclude the effects of differential uptake of the stimulus during MOI 10 inoculation of VERO-ZAP-WT cells, during VERO-ZAP-KO MOI 2 inoculation we added heat-inactivated Zika virus equivalent of MOI 8. After extensive washing and 72 h incubation, the same Zika antigen loads in VERO-ZAP-WT and VERO-ZAP-KO cells were confirmed with viral E protein staining (Figure 2(B)). The same Zika RNA loads in VERO-ZAP-WT and VERO-ZAP-KO cells were also confirmed using Zika-specific RT-qPCR and next-generation-sequencing (NGS) in sonicated cellular lysates (input) and immunoprecipitated viral RNA–protein complexes (enriched) (Figures 2(C,D)); Figure S4; Supplemental Dataset 1). High RT-qPCR Zika loads and nearly entire Zika genomic coverage with high NGS depth (Figures 2(C,D); Figure S4) confirms that the ChIRP method efficiently recovered the same high loads of viral RNA in both VERO-ZAP-WT and VERO-ZAP-KO cells. Also, as expected, viral RNA loads were consistently and considerably (around  $10^1$  difference) higher in enriched than in input samples in RT-qPCR and NGS assays (Figures 2(C,D); Figure S4). Altogether, we confirmed normalized viral loads and comparable enrichment of viral RNA during ChIRP in VERO-ZAP-WT and VERO-

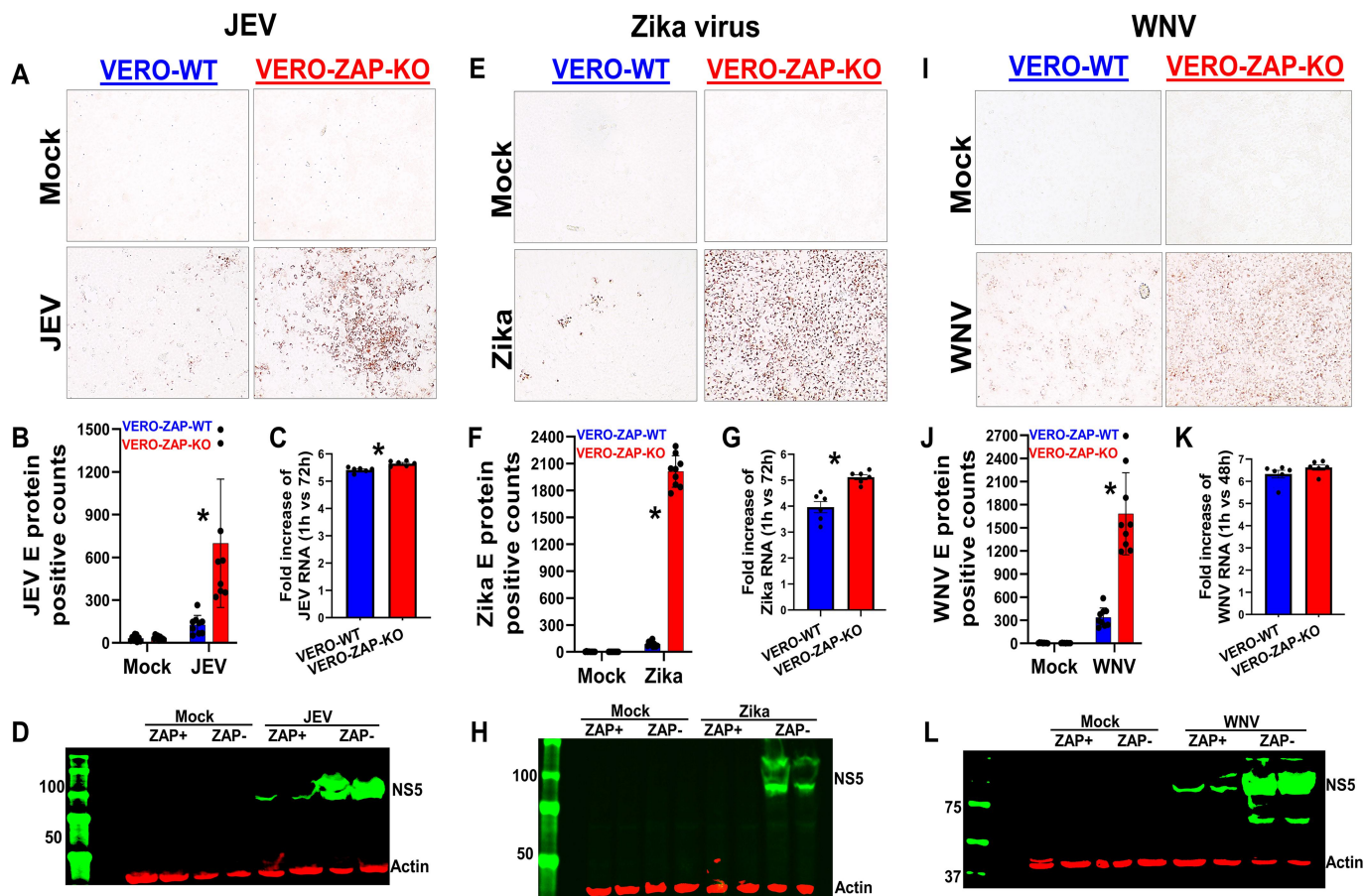


**Figure 1.** ZAP affects JEV, Zika, and WNV infection phenotypes. Representative images of cells positive for JEV (A), Zika virus (E), and WNV (I) E protein (red staining) at 72 h (48 h for WNV), MOI 0.01. Magnification x200. The experiment was done in 3 biological and 3 technical replicates. Figures represent the general patterns in all replicates. All 9 replicates for VERO-ZAP-WT and VERO-ZAP-KO cells are shown in Figure S1. The digital quantification of JEV (B), Zika (F), and WNV (J) positive cells in all 9 replicates from Figure S1. \*Unpaired t-test:  $P < 0.05$ . In mock-infected cells digital sensitive counting represents the staining background. The fold increase of JEV (C), Zika (G), and WNV (K) RNA loads in cell lysates collected at 1 h and 72 h (48 h for WNV) after inoculation. VERO-ZAP-WT and VERO-ZAP-KO cells were inoculated with MOI 0.01. Virus inoculums were removed and replaced with media. Cell lysates were collected with a lysis buffer at 1 h post-inoculation (to normalize for leftover virus inoculum RNA) and at 48–72 h. \*Unpaired t-test:  $P < 0.05$ . The experiment was done in 3 biological and 2 technical replicates. (D, H, L) reduced flavivirus infection in VERO-ZAP-WT cells at 72 h (48 h for WNV) represented by western blot for NS5 proteins. Normalized 50  $\mu$ g of protein was used for all samples. Two biological replicates for each condition are shown.

ZAP-KO cells, permitting quantitative comparison of proteins associated with viral RNA between wild-type and ZAP-KO cells.

Next, we used the Mass Spectrometry Interaction Statistics (MiST) to analyse raw ChIRP-MS data (Supplemental Dataset 2) previously applied in ChIRP-MS studies [11,33,34]. We employed MiST with default parameters and used the Singleton Filtering option to exclude proteins with spectral counts in only one biological replicate, quantifying proteins with a MiST score of 0.75 or above [11,33,34]. Additionally, we excluded proteins that had at least one spectral count in any biological replicate of mock-infected wild-type or ZAP-KO cells [11,32]. We applied three analytical strategies to analyse ChIRP-MS data (Table S1):

For the first analytical strategy, using the raw ChIRP-MS data with a total of 2,269 proteins (Table S1B), we identified proteins specifically associated with Zika virus RNA in VERO-ZAP-WT cells. We defined the resultant list of enriched proteins as the ‘extended’ Zika virus RNA interactome in VERO-ZAP-WT cells. This extended interactome contains 383 proteins (Table S1C). We named this

interactome ‘extended’ because additional control criteria were applied to narrow down and enrich the ‘ZAP-dependent’ Zika virus RNA interactome (see below).

ChIRP-MS is a rather new technique in molecular biology; the first time it was described for systemic identification of cellular proteins interacting with cellular mRNA in 2015 [7]. From 2019, several virology groups have applied ChIRP-MS to characterize interactions between cellular proteins and genomic RNA of severe acute respiratory syndrome coronavirus 2, Ebola virus, dengue virus, and Zika virus in wild-type ZAP-positive cells [8–11]. Thus, we compared our extended Zika virus RNA interactome in VERO-ZAP-WT cells with the Zika interactome in Huh cells from a previous publication [10]. A similar number of proteins were reported here—383, and previously—395. The comparison also showed a good reproducibility of 25.4% between two protein sets (Table S1D). We consider 25.4% a good reproducibility because studies were done in cells of different species – nonhuman primates (VERO) and humans (Huh), with different MOIs and sampling time points.

The specificity of our ChIRP-MS is also confirmed by physical associations between Zika virus RNA and viral prM, C, E, NS1,



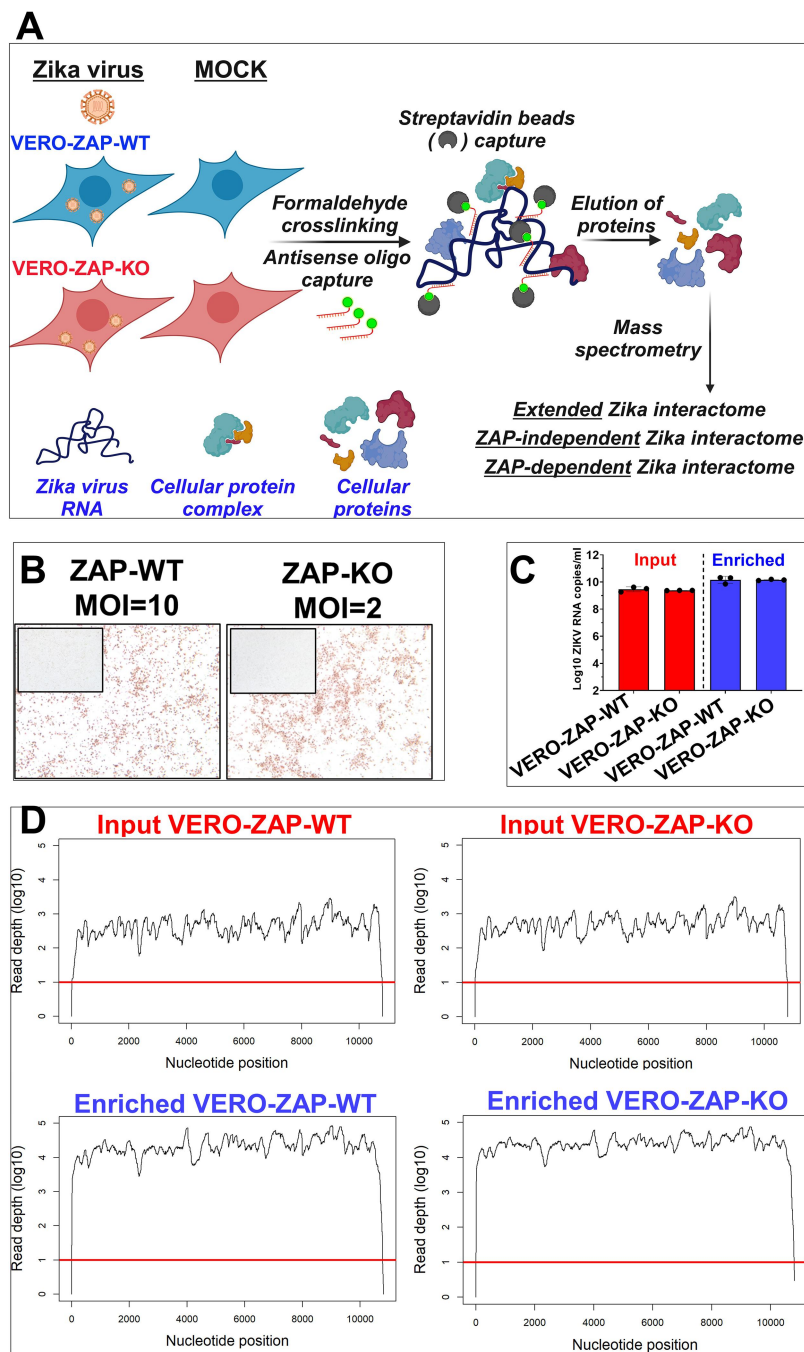


**Figure 2.** ChIRP-MS study design and validation. (A) ChIRP-MS experimental design to compare viral RNA-host protein interactions in zap-positive and ZAP-KO cells. ChIRP-MS was done in three biological replicates; each biological replicate consisted of lysed cells from four T-175 flasks for each experimental condition. (B) we adapted normalized MOIs to induce similar Zika viral loads in ZAP-WT and ZAP-KO cells. Red staining represents a similar number of Zika virus E protein-positive cells in WT and KO cells. Inserts – mock-infected cells. (C) the same Zika RNA loads in ZAP-WT and ZAP-KO cells were also confirmed using RT-qPCR. Input - sonicated cellular lysates. Enriched - immunoprecipitated viral RNA-protein complexes bound to MyOne C1 magnetic beads at the last washing step before protein elution. RNA was extracted from a 40  $\mu$ l of cell lysate or bead suspension in the washing buffer representing each biological replicate and subjected to Zika virus-specific RT-qPCR; dots represent ChIRP-MS biological replicates. (D) the same nearly entire Zika RNA genome coverage and NGS depth in ZAP-WT and ZAP-KO cells. Representative data from one ChIRP-MS biological replicate for ZAP-WT and ZAP-KO cells. Input and Enriched are the same sample types as for RT-qPCR in C. Control NGS in mock-infected cells did not show Zika-specific sequences (Figure S4). A red line shows the 10-nucleotide NGS depth threshold.

NS2A, NS2B, NS3, and NS5 proteins in only infected cells, while all mock-infected replicates were negative (Table S1E). The enrichment of viral proteins provides evidence that ChIRP-MS covers interactions across the entire length of viral RNA [8]. Analysis of the MiST abundance score and absolute spectral counts showed that the viral NS3 and NS5 proteins were most strongly recovered (Table S1E; NS3 MiST abundance score 0.167,

NS5 MiST abundance score 0.304; NS3 mean spectral counts 39, NS5 mean spectral counts 102), which is consistent with previous ChIRP-MS Zika virus study where NS3 and NS5 were also most abundant [10]; and with direct-binding function of flavivirus NS3—RNA helicase, and NS5—RNA-dependent RNA polymerase.

Analysis of top interacting cellular proteins with the highest spectral counts and GO enrichment analysis also suggested the

specificity of ChIRP-MS. All top 15 interacting proteins (except NCOA5) with the highest spectral counts (Figure 3(A)) are known factors of RNA biology, including RNA binding, RNA splicing, and RNA helicase activities (Table S1C). Gene Ontology enrichment analysis also showed that all seven

enriched pathways with at least two-fold enrichment represent nucleic acid/RNA binding and RNA biology processes (Figure 3(D)).

For the second analytical strategy, we identified proteins specifically interacting with Zika virus RNA in VERO-ZAP-KO cells.

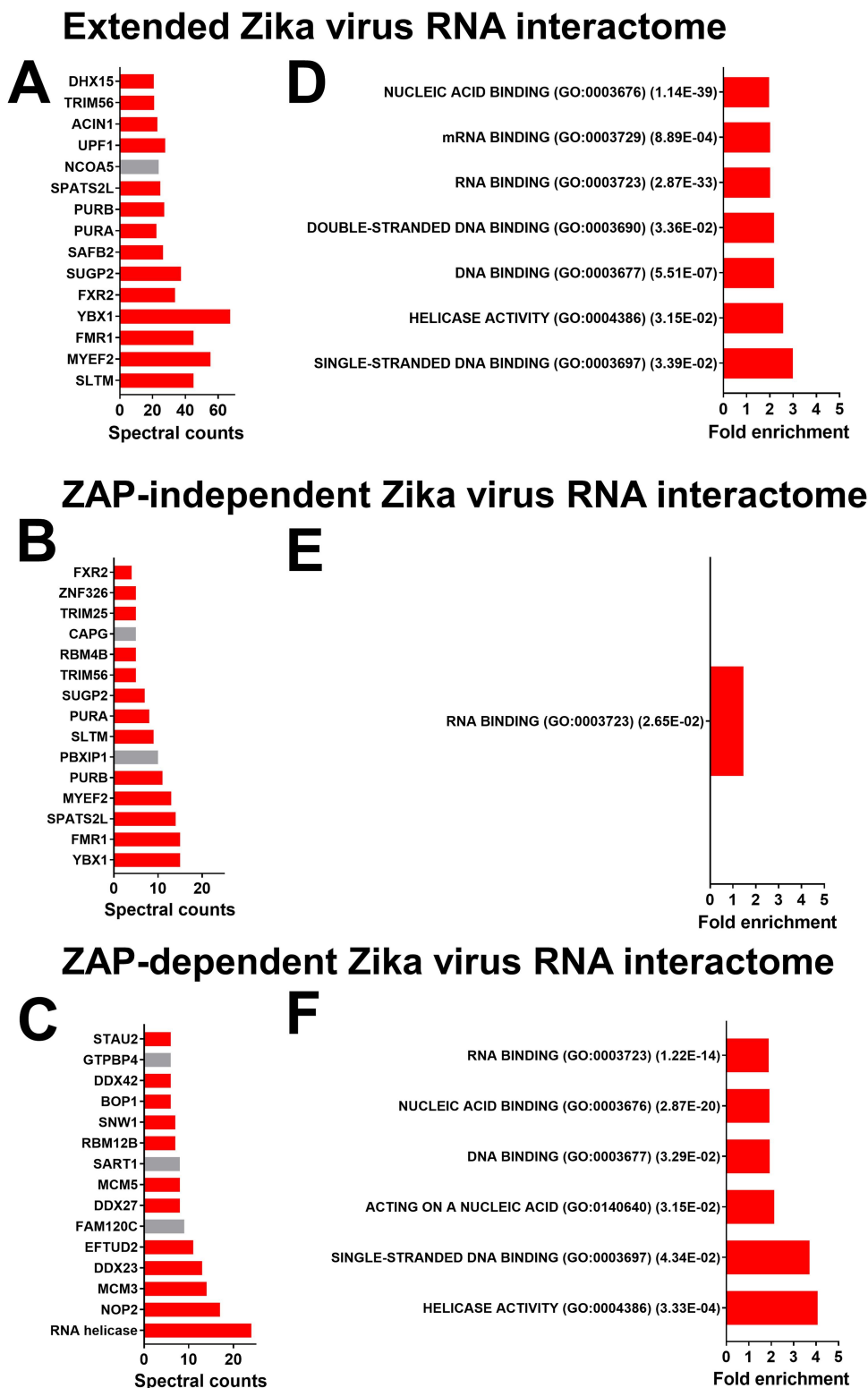


**Figure 3.** Top ChIRP-MS proteins and GO pathways identified in the extended, ZAP-independent, and ZAP-dependent Zika virus RNA interactomes. Mean spectral counts are shown for proteins in (A, B, C). Spectral counts for all three biological replicates are shown in tables S1C, F, H. The top proteins with unknown functions in RNA biology are highlighted in grey. For GO pathways in (D, E, F), GO identification numbers and FDR-adjusted *P* values are shown in parentheses. All GO processes were overrepresented.

For specificity, we applied the same strategy as above: We selected the Singleton Filtering MiST option to exclude proteins with spectral counts in only one biological replicate and quantify proteins with the MiST score of 0.75 or above [11,33,34]. We also excluded all proteins with a single spectral count in at least one of the three biological replicates in mock-infected wild-type or ZAP-KO cells. We defined the resultant list of enriched proteins as a ‘ZAP-independent’ Zika virus RNA interactome. We defined this interactome as ZAP-independent because associated cellular proteins were discovered in VERO-ZAP-KO cells showing the ZAP-independent nature of interactions. The ZAP-independent interactome contains 116 proteins (Table S1F). As expected, most, 13 out of 15 top cellular interacting proteins with the highest spectral counts are known factors in RNA biology (Figure 3(B); Table S1F). Zika virus proteins were identified in only infected VERO-ZAP-KO cells (Table S1G).

Finally, to discover the ‘ZAP-dependent’ Zika RNA interactome in VERO-ZAP-WT cells, in addition to the above specificity exclusion criteria in MiST settings and mock-infected cells, we excluded proteins that had at least one spectral count in at least one of the three biological replicates in VERO-ZAP-KO cells infected with Zika virus. The ZAP-dependent interactome contains 209 proteins (Table S1H). The ZAP-dependent Zika RNA interactome has more proteins than ZAP-independent—209 versus 116 proteins. The difference in 93 proteins between interactomes in ZAP-WT and ZAP-KO cells is rational because in the previous study a tandem mass spectrometry showed that 114 cellular proteins interact with the overexpressed immunoprecipitated ZAP large isoform in uninfected cells [32]. Other large-scale interactome studies in uninfected cells have identified more than 250 potential cellular proteins that may potentially interact with ZAP [32,35–38].

As expected, most, 12 out of 15 top interacting proteins with the highest spectral counts in the ZAP-dependent interactome are known factors in RNA biology (Figure 3(C); Table S1H). Comparative GO enrichment analysis between ZAP-independent and ZAP-dependent interactomes showed only one enriched pathway related to RNA biology in ZAP-KO cells and six enriched RNA biology pathways in ZAP-WT cells, including ‘helicase activity’ with the highest fold enrichment (Figures 3(E,F)). Accordingly, among the top 15 proteins in the ZAP-dependent interactome, four proteins were RNA helicases (Table S1H). In total, 11 RNA helicases were enriched in the ZAP-dependent interactome – DDX42, DDX56, DDX27, DDX50, DDX52, DDX23, DDX54, DDX18, DHX57, DDX47, and one uncharacterized RNA helicase (Tables S1H, I).

Altogether, using ChIRP-MS and MiST analysis, we characterized the cellular interactome associated with Zika virus RNA, including Extended, ZAP-independent, and ZAP-dependent interactomes.

### **ZAP wild-type and knockout VERO cells express DDX RNA helicases**

ZAP binds cellular mRNA and affects gene expression, including antiviral and immune resolution transcriptional responses [39,40]. Thus, it was unclear whether the enrichment of RNA helicases in the ChIRP ZAP-dependent Zika interactome (Tables S1H; Figures 3(C,F)) and the depletion

of RNA helicases in the ChIRP ZAP-independent Zika interactome (Tables S1F; Figures 3(B,E)) were exclusively due to direct ZAP-viral RNA-cellular RNA helicase interactions in ZAP-WT cells and the lack of such interactions in ZAP-KO cells or ZAP-mediated effects on cellular RNA helicase mRNAs also played a role. Therefore, we quantified the protein levels of four selected helicases (DDX23, DDX27, DDX42, and DDX50) using Western blot in MOCK and infected ZAP-WT and ZAP-KO cells (the same MOI and sampling time as for the ChIRP-MS experiment). DDX42 and DDX27 were chosen because they were among the top three enriched helicases (Table S1I). DDX23 and DDX50 are known to have antiviral activity [41,42].

Western blot analysis revealed expression of all four RNA helicases in both VERO-ZAP-KO and VERO-ZAP-WT cells, under mock condition and during Zika virus infection (Figure 4(A)). The expression of DDX23 and DDX27 was lower in both MOCK and Zika virus-infected ZAP-KO cells compared to ZAP-WT cells (DDX23  $p = 0.0374$ ;  $p = 0.0471$ ; DDX27  $p < 0.0001$ ;  $p = 0.0004$ ), although ZAP-KO cells still showed prominent DDX23 and DDX27 expression (Figures 4(A,B)). Zika virus infection significantly reduced DDX27 expression in both cell lines (ZAP-KO  $p = 0.415$ ; ZAP-WT  $p = 0.001$ ) (Figure 4(A,B)). The expression of DDX42 was significantly lower in mock-infected ZAP-WT than in ZAP-KO cells ( $p = 0.0179$ ). Zika virus infection considerably reduced DDX42 expression in both cell lines, but the comparative expression in ZAP-KO and ZAP-WT cells during infection was similar ( $p = 0.2139$ ) (Figures 4(A,B)). The expression of DDX50 was lower in both MOCK and Zika virus-infected ZAP-KO cells compared to ZAP-WT cells (MOCK  $p = 0.0001$ ; Zika  $p < 0.0001$ ), although ZAP-KO cells still showed prominent DDX50 expression (Figures 4(A,B)). The Zika virus infection did not affect DDX50 expression in either cell line (Figures 4(A,B)).

Overall, we confirmed that ZAP-WT and ZAP-KO cells express all four tested RNA helicases – DDX23, DDX27, DDX42 and DDX50. However, ZAP knockout was associated with reduced DDX23, DDX27, and DDX50 expression in both MOCK and infection conditions. These reduced cellular expressions of DDX23, DDX27 and DDX50 suggest that ZAP-mediated effects on cellular RNA helicase mRNAs may contribute to the depletion of RNA helicases in the ChIRP ZAP-independent Zika interactome. In contrast, DDX42 expression was even in ZAP-KO and ZAP-WT cells during Zika virus infection, indicating that direct interactions between ZAP, viral RNA, and cellular RNA helicases in ZAP-WT cells may play the central role in the enrichment of RNA helicases in the ChIRP ZAP-dependent Zika interactome.

### **Discussion**

All previous ChIRP-MS studies on a viral RNA-cellular protein interactome were done in wild-type cell lines [8–11], and comparative ChIRP-MS studies in wild-type and KO cells were not reported. Here, using ChIRP-MS in ZAP-WT and

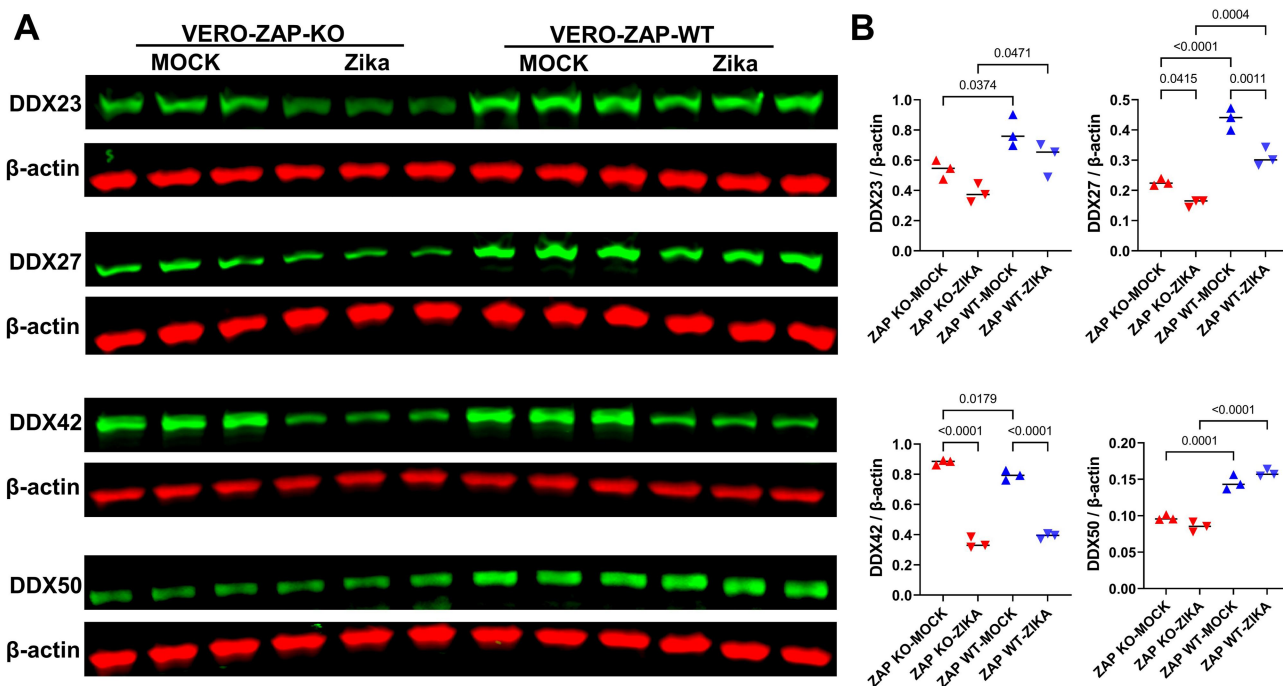


**Figure 4.** The expression of RNA helicases in VERO-ZAP-WT and VERO-ZAP-KO cells. Cells were mock infected or infected with normalized Zika virus MOIs; MOI 2 or 10 for VERO-ZAP-KO and VERO-ZAP-WT cells, respectively, as described for ChIRP in supplemental materials and methods. Cells were sampled at 72 h after mock or virus infection. **(A)** green bands represent DDX23 (96 kDa), DDX27 (90 kDa), DDX42 (117-120 kDa), and DDX50 (83 kDa) RNA helicases. Red bands represent  $\beta$ -actin loading control (42 kDa). Western blot was done in 3 biological replicates for each experimental condition. **(B)** the expression of DDX RNA helicases was quantified as described in supplemental material and methods.

ZAP-KO cells, we delineated ZAP-independent and ZAP-dependent cellular protein interactomes associated with Zika virus RNA. We showed that such experimental approach is feasible by normalizing MOIs and viral loads in ZAP-WT and ZAP-KO cells. Despite extensive research on ZAP's antiviral activity, to our knowledge, this study is the first to explore the ZAP-dependent interactome specifically associated with viral RNA.

ZAP requires RNA helicases as co-factors: ZAP's N-terminus interacts with the N- and C-terminal domains of DDX17 that promotes ZAP-mediated degradation of murine leukaemia reporter virus [43]. However, our ChIRP-MS Zika data do not contain p72 DEAD-box RNA helicase (DDX17) (Table S1B). DHX30 interacts with ZAP, and the knockdown of DHX30 reduces ZAP's antiviral activity against murine leukaemia reporter virus [44]. Accordingly, we identified DHX30 in ChIRP-MS data (Table S1B); however, it was excluded from further interactome-specific analysis with our rigorous specificity cut-off. Interestingly, we found that 11 RNA helicases were enriched in the ZAP-dependent interactome – DDX42, DDX56, DDX27, DDX50, DDX52, DDX23, DDX54, DDX18, DHX57, DDX47, and one uncharacterized RNA helicase. In contrast, in the ZAP-independent interactome, no RNA helicases were enriched. The limitation is that our experimental design does not allow to identify the specific nature of interactions between Zika virus RNA and cellular proteins. We do not know yet which cellular proteins interact with only ZAP bound to viral RNA, which interact with ZAP and viral RNA, and which proteins have strict viral RNA dependency during interactions with ZAP. ZAP binds to

single-stranded viral RNA and potentially to single overhangs in double-stranded RNA [45,46]; RNA helicases can bind to double-stranded RNA, single overhangs in double-stranded RNA and single-stranded RNA; these make interactions between ZAP, viral RNA, and RNA helicases spatially possible. Additional research is necessary to determine if the RNA helicases identified in this study function as co-factors for ZAP in its antiviral activity, specifically ZAP-mediated degradation of viral RNA.

In addition to RNA helicases, ZAP requires other co-factors. It lacks intrinsic RNase activity but recruits the 5' and 3' RNA degradation machinery [24,47]. The E3 ubiquitin ligase TRIM25 is important for ZAP activity against alphaviruses by increasing inhibition of viral translation [48,49]. ZAP also interacts with the cytoplasmic protein KHNYN to inhibit CpG-enriched HIV-1 [50]. Riplet, a protein known to play a central role in activating the retinoic acid-inducible gene I (RIG-I), has been recently identified as a ZAP co-factor that augments the restriction of HIV-1 [51]. However, the full complexity of cellular proteins essential for ZAP antiviral activity is unknown. Large-scale interactome studies in non-infected cells have identified more than 250 proteins that may interact with ZAP [32,35–38]. Notably, there were no large-scale ZAP interactome studies in the context of viral infection [35]. Thus, our ZAP-dependent ChIRP-MS interactome (Table S1H) provides a highly specific list of potential ZAP co-factors, including 11 RNA helicases for future mechanistic and functional studies.

It is known that DDX RNA helicases not only facilitate viral RNA degradation but also act as viral RNA sensing proteins contributing to cellular innate immune signalling,



type I IFN production, and antiviral response [52–57]. Also, viruses can abduct cellular RNA helicases to support their lifecycle and promote infectivity [58,59]. Cellular RNA helicases often interact with microbial genomes and evoke their properties in the complex with different adaptor proteins [52–54,56,60–62]. Thus, ZAP may play a dual role in mediating RNA helicase-dependent antiviral and proviral effects. Before our ChIRP-MS study, such co-factor/adaptor role of ZAP in interactions between viral RNA and cellular RNA helicases was not considered.

Interestingly, Western blot analysis showed that ZAP expression is associated with higher levels of at least three RNA helicases—DDX23, DDX27 and DDX50—since their expression was reduced in both MOCK and infected ZAP-KO cells as compared to ZAP-WT cells (Figure 4). Thus, ZAP may indirectly contribute to antiviral cellular responses by maintaining the expression of RNA helicases, which are known to have antiviral activity, including DDX23 and DDX50 [41,42].

Another interesting finding is that Zika virus infection considerably reduced the expression of DDX23, DDX27 and DDX42 in ZAP-WT cells (Figure 4), as well as ZAP (Figure S3) under our experimental conditions (72 h post-infection). These observations may indicate Zika virus strategies for evading cellular immune responses, warranting further investigation.

The primary limitation of this study is its focus on an associative ChIRP-MS comparison between ZAP-WT and ZAP-KO cells. While conducting functional studies could provide further insights, it falls beyond the scope of this work. Nonetheless, our ZAP-dependent interactome offers the scientific community a valuable resource for future studies on ZAP, its co-factors, and viral RNA interactions. It would also be interesting to compare ChIRP-MS interactomes across different ZAP-WT and ZAP-KO cell lines infected with various viruses. Our strict filtering approach to identify the ZAP-dependent interactome, which excluded proteins from the ZAP-independent interactome even with a single MS spectral count in ZAP-KO cells, might be seen as too rigorous. However, it ensures a highly specific list of potential ZAP co-factors. Additionally, we have made available the raw and extended ZAP interactome databases (Table S1B, C; Supplemental Dataset 2), allowing others to apply their own filtering approaches.

## Conclusions

Together, the ZAP-dependent interactome identified with ChIRP-MS provides potential ZAP co-factors for antiviral activity against Zika virus and possibly other viruses. Identifying the full spectrum of ZAP co-factors and mechanisms of how they act will be critical to understand the ZAP antiviral system and may contribute to the development of antivirals.

## Materials and methods

Details of ChIRP-MS, cells, viruses, comparative infection studies, RT-qPCR, Western blot, and statistics are in Supplemental Materials and Methods.

## Disclosure statement

No potential conflict of interest was reported by the author(s).

## Funding

PPS received a Scholarship from the School of Public Health, University of Saskatchewan. This work was partially supported by a grant to UK from the Canadian Institutes of Health Research [CIHR; Project Grant #424307]. The funders had no role in study design, data collection and analysis, decision to publish, or manuscript preparation.

## Author contributions

Conceptualization: UK. Investigation: NPKL, AJS, PPS, UK. Data analysis: NPKL, AJS, PPS, UK. Funding: UK. Resources: UK. Writing – original draft preparation: NPKL, AJS, PPS, UK. Writing – review and editing: UK, NPKL, PPS.

## Data availability statement

Data available within the article, its supplementary materials and DRYAD open data publishing platform which can be accessed via links: <https://doi.org/10.5061/dryad.280gb5mz5> and <https://doi.org/10.5061/dryad.kwh70rzd1>.

## ORCID

Uladzimir Karniychuk  <http://orcid.org/0000-0001-7802-9223>

## References

- [1] Amicizia D, Zangrillo F, Lai PL, et al. Overview of Japanese encephalitis disease and its prevention. Focus on IC51 vaccine (IXIARO®). *J Preventative Med Hygiene*. 2018;59:E99–E107.
- [2] Tarantola A, Goutard F, Newton P, et al. Estimating the burden of Japanese encephalitis virus and other encephalitides in countries of the mekong region. *PLOS Negl Trop Dis*. 2014;81:e2533. doi: [10.1371/journal.pntd.0002533](https://doi.org/10.1371/journal.pntd.0002533)
- [3] Oliveira ARS, Piaggio J, Cohnstaedt LW, et al. Introduction of the Japanese encephalitis virus (JEV) in the United States – a qualitative risk assessment. *Transbound Emerg Dis*. 2019;66(4):1558–1574. doi: [10.1111/tbed.13181](https://doi.org/10.1111/tbed.13181)
- [4] Huang YJS, Harbin JN, Hettenbach SM, et al. Susceptibility of a North American culex quinquefasciatus to Japanese encephalitis virus. *Vector borne and zoonotic diseases*. (Larchmont, N.Y.): Vector Borne Zoonotic Dis; 2015. p. 709–711.
- [5] Faizah AN, Kobayashi D, Matsumura R, et al. Blood meal source identification and RNA virome determination in Japanese encephalitis virus vectors collected in Ishikawa prefecture, Japan, show distinct avian/mammalian host preference. *J Med Entomol*. [2023 Apr 7];60(3):620–628. doi: [10.1093/jme/tjad028](https://doi.org/10.1093/jme/tjad028)
- [6] Howard-Jones AR, Pham D, Jeoffreys N, et al. Emerging genotype IV Japanese encephalitis virus outbreak in New South Wales, Australia. *Viruses*. [2022 Aug 24];14(9):1853. doi: [10.3390/v14091853](https://doi.org/10.3390/v14091853)
- [7] Chu C, Zhang QC, da Rocha ST, et al. Systematic discovery of xist RNA binding proteins. *Cell*. [2015 Apr 9];161(2):404–416. doi: [10.1016/j.cell.2015.03.025](https://doi.org/10.1016/j.cell.2015.03.025)
- [8] Flynn RA, Belk JA, Qi Y, et al. Discovery and functional interrogation of SARS-CoV-2 RNA-host protein interactions. *Cell*. [2021 Apr 29];184(9):2394–2411.e16. doi: [10.1016/j.cell.2021.03.012](https://doi.org/10.1016/j.cell.2021.03.012)
- [9] Labeau A, Fery-Simonian L, Lefevre-Utile A, et al. Characterization and functional interrogation of the SARS-CoV-2 RNA interactome. *Cell Rep*. [2022 Apr 26];39(4):110744. doi: [10.1016/j.celrep.2022.110744](https://doi.org/10.1016/j.celrep.2022.110744)



- [10] Ooi YS, Majzoub K, Flynn RA, et al. An RNA-centric dissection of host complexes controlling flavivirus infection. *Nat Microbiol.* 2019 Dec;4(12):2369–2382. doi: [10.1038/s41564-019-0518-2](https://doi.org/10.1038/s41564-019-0518-2)
- [11] Zhang S, Huang W, Ren L, et al. Comparison of viral RNA-host protein interactomes across pathogenic RNA viruses informs rapid antiviral drug discovery for SARS-CoV-2. *Cell Res.* 2022 Jan;32(1):9–23. doi: [10.1038/s41422-021-00581-y](https://doi.org/10.1038/s41422-021-00581-y)
- [12] Gao G, Guo X, Goff SP. Inhibition of retroviral RNA production by ZAP, a cch-type zinc finger protein. *Science.* 2002;297(5587):1703–1706. doi: [10.1126/science.1074276](https://doi.org/10.1126/science.1074276)
- [13] Bick MJ, Carroll JW, Gao G, et al. Expression of the zinc-finger antiviral protein inhibits alphavirus replication. *J Virol.* 2003 Nov;77(21):11555–11562. doi: [10.1128/JVI.77.21.11555-11562.2003](https://doi.org/10.1128/JVI.77.21.11555-11562.2003)
- [14] Nguyen LP, Aldana KS, Yang E, et al. Alphavirus evasion of zinc finger antiviral protein (ZAP) correlates with CpG suppression in a specific viral nsP2 gene sequence. *Viruses.* [2023 Mar 24];15(4):830. doi: [10.3390/v15040830](https://doi.org/10.3390/v15040830)
- [15] Liu CH, Zhou L, Chen G, et al. Battle between influenza A virus and a newly identified antiviral activity of the parp-containing ZAPL protein. *Proc Natl Acad Sci U S A.* [2015 Nov 10];112(45):14048–14053. doi: [10.1073/pnas.1509745112](https://doi.org/10.1073/pnas.1509745112)
- [16] Mao R, Nie H, Cai D, et al. Inhibition of hepatitis B virus replication by the host zinc finger antiviral protein. *PloS Pathog.* 2013;9(7):e1003494. doi: [10.1371/journal.ppat.1003494](https://doi.org/10.1371/journal.ppat.1003494)
- [17] Muller S, Moller P, Bick MJ, et al. Inhibition of filovirus replication by the zinc finger antiviral protein. *J Virol.* 2007 Mar;81(5):2391–2400. doi: [10.1128/JVI.01601-06](https://doi.org/10.1128/JVI.01601-06)
- [18] Tang Q, Wang X, Gao G, et al. The short form of the zinc finger antiviral protein inhibits influenza A virus protein expression and is antagonized by the virus-encoded NS1. *J Virol.* [2017 Jan 15];91(2). doi: [10.1128/JVI.01909-16](https://doi.org/10.1128/JVI.01909-16)
- [19] Zhu Y, Chen G, Lv F, et al. Zinc-finger antiviral protein inhibits HIV-1 infection by selectively targeting multiply spliced viral mRNAs for degradation. *Proc Natl Acad Sci USA.* [2011 Sep 20];108(38):15834–15839. doi: [10.1073/pnas.1101676108](https://doi.org/10.1073/pnas.1101676108)
- [20] Takata MA, Goncalves-Carneiro D, Zang TM, et al. CG dinucleotide suppression enables antiviral defence targeting non-self RNA. *Nature.* [2017 Oct 5];550(7674):124–127. doi: [10.1038/nature24039](https://doi.org/10.1038/nature24039)
- [21] Miyazato P, Matsuo M, Tan BJY, et al. HTLV-1 contains a high CG dinucleotide content and is susceptible to the host antiviral protein ZAP. *Retrovirology.* [2019 Dec 16];16(1):38. doi: [10.1186/s12977-019-0500-3](https://doi.org/10.1186/s12977-019-0500-3)
- [22] Gonzalez-Perez AC, Stempel M, Wyler E, et al. The zinc finger antiviral protein ZAP restricts human cytomegalovirus and selectively binds and destabilizes viral UL4/UL5 transcripts. *MBio.* [2021 May 4];12(3). doi: [10.1128/mBio.02683-20](https://doi.org/10.1128/mBio.02683-20)
- [23] Zhao Y, Song Z, Bai J, et al. ZAP, a CCCH-Type zinc finger protein, inhibits porcine reproductive and respiratory syndrome virus replication and interacts with viral Nsp9. *J Virol.* [2019 May 15];93(10). doi: [10.1128/JVI.00001-19](https://doi.org/10.1128/JVI.00001-19)
- [24] Chiu HP, Chiu H, Yang CF, et al. Inhibition of Japanese encephalitis virus infection by the host zinc-finger antiviral protein. *PLOS Pathogens: Public Library of Science;* 2018.
- [25] Fros JJ, Visser I, Tang B, et al. The dinucleotide composition of the zika virus genome is shaped by conflicting evolutionary pressures in mammalian hosts and mosquito vectors. *PLOS Biol.* 2021 Apr;19(4):e3001201. doi: [10.1371/journal.pbio.3001201](https://doi.org/10.1371/journal.pbio.3001201)
- [26] Phuong Khanh Le N, Pal Singh P, Jawad Sabir A, et al. Endogenous ZAP is associated with altered global cellular gene expression during Zika virus infection. *bioRxiv.* 2024. doi: [10.1101/2024.05.23.595518](https://doi.org/10.1101/2024.05.23.595518)
- [27] Pallett MA, Lu Y, Smith GL. DDX50 is a viral restriction factor that enhances IRF3 activation. *Viruses.* [2022 Feb 3];14(2):316. doi: [10.3390/v14020316](https://doi.org/10.3390/v14020316)
- [28] Buechler CR, Bailey AL, Weiler AM, et al. Seroprevalence of zika virus in wild African green monkeys and baboons. *mSphere.* 2017 Mar-Apr;2(2). doi: [10.1128/mSphere.00392-16](https://doi.org/10.1128/mSphere.00392-16)
- [29] Kerns JA, Emerman M, Malik HS, et al. Positive selection and increased antiviral activity associated with the parp-containing isoform of human zinc-finger antiviral protein. *PloS Genet.* 2008 Jan;4(1):e21. doi: [10.1371/journal.pgen.0040021](https://doi.org/10.1371/journal.pgen.0040021)
- [30] Goncalves-Carneiro D, Takata MA, Ong H, et al. Origin and evolution of the zinc finger antiviral protein. *PLOS Pathog.* 2021 Apr;17(4):e1009545. doi: [10.1371/journal.ppat.1009545](https://doi.org/10.1371/journal.ppat.1009545)
- [31] Li MMH, Aguilar EG, Michailidis E, et al. Characterization of novel splice variants of zinc finger antiviral protein (ZAP). *J Virol.* [2019 Sep 15];93(18). doi: [10.1128/JVI.00715-19](https://doi.org/10.1128/JVI.00715-19)
- [32] Goodier JL, Pereira GC, Cheung LE, et al. The broad-spectrum antiviral protein ZAP restricts human retrotransposition. *PLOS Genetics: Public Library of Science;* 2015. p. e1005252.
- [33] Verschueren E, Von Dollen J, Cimermancic P, et al. Scoring large-scale affinity purification mass spectrometry datasets with MiST. *Curr Protoc Bioinformatics.* [2015 Mar 9];49(8):19–18. doi: [10.1002/0471250953.bi0819s49](https://doi.org/10.1002/0471250953.bi0819s49)
- [34] Jager S, Cimermancic P, Gulbahce N, et al. Global landscape of hiv-human protein complexes. *Nature.* [2011 Dec 21];481(7381):365–370. doi: [10.1038/nature10719](https://doi.org/10.1038/nature10719)
- [35] Ficarelli M, Neil SJD, Swanson CM. Targeted restriction of viral gene expression and replication by the ZAP antiviral system. *Annu Rev Virol.* [2021 Sep 29];8(1):265–283. doi: [10.1146/annurev-virology-091919-104213](https://doi.org/10.1146/annurev-virology-091919-104213)
- [36] Caudron-Herger M, Rusin SF, Adamo ME, et al. R-Deep: proteome-wide and quantitative identification of RNA-Dependent proteins by density gradient ultracentrifugation. *Mol Cell.* [2019 Jul 11];75(1):184–199. doi: [10.1016/j.molcel.2019.04.018](https://doi.org/10.1016/j.molcel.2019.04.018)
- [37] Huttlin EL, Bruckner RJ, Paulo JA, et al. Architecture of the human interactome defines protein communities and disease networks. *Nature.* [2017 May 25];545(7655):505–509. doi: [10.1038/nature22366](https://doi.org/10.1038/nature22366)
- [38] Youn JY, Dunham WH, Hong SJ, et al. High-density proximity mapping reveals the subcellular organization of mRNA-associated granules and bodies. *Mol Cell.* [2018 Feb 1];69(3):517–532. doi: [10.1016/j.molcel.2017.12.020](https://doi.org/10.1016/j.molcel.2017.12.020)
- [39] Todorova T, Bock FJ, Chang P. PARP13 regulates cellular mRNA post-transcriptionally and functions as a pro-apoptotic factor by destabilizing TRAILR4 transcript. *Nat Commun.* [2014 Nov 10];5(1):5362. doi: [10.1038/ncomms6362](https://doi.org/10.1038/ncomms6362)
- [40] Schwerk J, Soveg FW, Ryan AP, et al. RNA-binding protein isoforms zap-S and ZAP-L have distinct antiviral and immune resolution functions. *Nat Immunol.* 2019 Dec;20(12):1610–1620. doi: [10.1038/s41590-019-0527-6](https://doi.org/10.1038/s41590-019-0527-6)
- [41] Abdullah SW, Han S, Wu J, et al. The DDX23 negatively regulates translation and replication of foot-and-mouth disease virus and is degraded by 3C proteinase. *Viruses.* [2020 Nov 25];12(12):1348. doi: [10.3390/v12121348](https://doi.org/10.3390/v12121348)
- [42] Han P, Ye W, Lv X, et al. DDX50 inhibits the replication of dengue virus 2 by upregulating ifn-beta production. *Arch Virol.* 2017 Jun;162(6):1487–1494. doi: [10.1007/s00705-017-3250-3](https://doi.org/10.1007/s00705-017-3250-3)
- [43] Chen G, Guo X, Lv F, et al. p72 DEAD box RNA helicase is required for optimal function of the zinc-finger antiviral protein. *Proc Natl Acad Sci U S A.* [2008 Mar 18];105(11):4352–4357. doi: [10.1073/pnas.0712276105](https://doi.org/10.1073/pnas.0712276105)
- [44] Ye P, Liu S, Zhu Y, et al. DEXH-Box protein DHX30 is required for optimal function of the zinc-finger antiviral protein. *Protein Cell.* 2010 Oct;1(10):956–964. doi: [10.1007/s13238-010-0117-8](https://doi.org/10.1007/s13238-010-0117-8)
- [45] Xu S, Ci Y, Wang L, et al. Zika virus NS3 is a canonical RNA helicase stimulated by NS5 RNA polymerase. *Nucleic Acids Res.* [2019 Sep 19];47(16):8693–8707. doi: [10.1093/nar/gkz650](https://doi.org/10.1093/nar/gkz650)
- [46] Luo X, Wang X, Gao Y, et al. Molecular mechanism of RNA recognition by zinc-finger antiviral protein. *Cell Rep.* [2020 Jan 7];30(1):46–52. doi: [10.1016/j.celrep.2019.11.116](https://doi.org/10.1016/j.celrep.2019.11.116)
- [47] Zhu Y, Gao G. Zap-mediated mRNA degradation. *RNA Biol.* 2008 Apr-Jun;5(2):65–67. doi: [10.4161/rna.5.2.6044](https://doi.org/10.4161/rna.5.2.6044)
- [48] Li MM, Lau Z, Cheung P, et al. TRIM25 enhances the antiviral action of zinc-finger antiviral protein (ZAP). *PloS Pathog.* 2017 Jan;13(1):e1006145. doi: [10.1371/journal.ppat.1006145](https://doi.org/10.1371/journal.ppat.1006145)
- [49] Zheng X, Wang X, Tu F, et al. TRIM25 is required for the antiviral activity of zinc finger antiviral protein. *J Virol.* 2017;91(9). doi: [10.1128/JVI.00088-17](https://doi.org/10.1128/JVI.00088-17)

- [50] Ficarelli M, Wilson H, Pedro Galão R, et al. KHNYN is essential for the zinc finger antiviral protein (ZAP) to restrict HIV-1 containing clustered CpG dinucleotides. *eLife*; 2019.
- [51] Buckmaster MV, Goff SP. Ripler binds the zinc finger antiviral protein (ZAP) and augments ZAP-Mediated restriction of HIV-1. *J Virol*. 2022;96(16):e0052622. doi: [10.1128/jvi.00526-22](https://doi.org/10.1128/jvi.00526-22)
- [52] Zhang Z, Kim T, Bao M, et al. DDX1, DDX21, and DHX36 helicases form a complex with the adaptor molecule TRIF to sense dsRNA in dendritic cells. *Immunity*. [2011 Jun 24];34(6):866–878. doi: [10.1016/j.immuni.2011.03.027](https://doi.org/10.1016/j.immuni.2011.03.027)
- [53] Kim T, Pazhoor S, Bao M, et al. Aspartate-glutamate-alanine-histidine box motif (DEAH)/RNA helicase a helicases sense microbial DNA in human plasmacytoid dendritic cells. *Proc Natl Acad Sci USA*. [2010 Aug 24];107(34):15181–15186. doi: [10.1073/pnas.1006539107](https://doi.org/10.1073/pnas.1006539107)
- [54] Zhang Z, Yuan B, Lu N, et al. DHX9 pairs with IPS-1 to sense double-stranded RNA in myeloid dendritic cells. *J Immunol*. [2011 Nov 1];187(9):4501–4508. doi: [10.4049/jimmunol.1101307](https://doi.org/10.4049/jimmunol.1101307)
- [55] Patabhi S, Knoll ML, Gale M Jr., et al. DHX15 is a coreceptor for RLR signaling that promotes antiviral defense against RNA virus infection. *J Interferon Cytokine Res*. 2019 Jun;39(6):331–346. doi: [10.1089/jir.2018.0163](https://doi.org/10.1089/jir.2018.0163)
- [56] Miyashita M, Oshiumi H, Matsumoto M, et al. DDX60, a DEXD/H box helicase, is a novel antiviral factor promoting RIG-I-like receptor-mediated signaling. *Mol Cell Biol*. 2011 Sep;31(18):3802–3819. doi: [10.1128/MCB.01368-10](https://doi.org/10.1128/MCB.01368-10)
- [57] Ermler ME, Yerukhim E, Schriewer J, et al. RNA helicase signaling is critical for type I interferon production and protection against rift valley fever virus during mucosal challenge. *J Virol*. 2013 May;87(9):4846–4860. doi: [10.1128/JVI.01997-12](https://doi.org/10.1128/JVI.01997-12)
- [58] Steimer L, Klostermeier D. RNA helicases in infection and disease. *RNA Biol*. 2012 Jun;9(6):751–771. doi: [10.4161/rna.20090](https://doi.org/10.4161/rna.20090)
- [59] Wu CY, Nagy PD, Wang A. Role reversal of functional identity in host factors: dissecting features affecting pro-viral versus antiviral functions of cellular dead-box helicases in tombusvirus replication. *PLOS Pathog*. 2020 Oct;16(10):e1008990. doi: [10.1371/journal.ppat.1008990](https://doi.org/10.1371/journal.ppat.1008990)
- [60] Cheng W, Chen G, Jia H, et al. DDX5 RNA helicases: emerging roles in viral infection. *Int J Mol Sci*. [2018 Apr 9];19(4):1122. doi: [10.3390/ijms19041122](https://doi.org/10.3390/ijms19041122)
- [61] Mitoma H, Hanabuchi S, Kim T, et al. The DHX33 RNA helicase senses cytosolic RNA and activates the NLRP3 inflammasome. *Immunity*. [2013 Jul 25];39(1):123–135. doi: [10.1016/j.immuni.2013.07.001](https://doi.org/10.1016/j.immuni.2013.07.001)
- [62] Zhang Z, Yuan B, Bao M, et al. The helicase DDX41 senses intracellular DNA mediated by the adaptor STING in dendritic cells. *Nat Immunol*. [2011 Sep 4];12(10):959–965. doi: [10.1038/ni.2091](https://doi.org/10.1038/ni.2091)